

Optical Phonon Modes and Dielectric Behavior of $\text{Sr}_{1-3x/2}\text{Ce}_x\text{TiO}_3$ Microwave Ceramics

Roberto L. Moreira,^{*,†} Ricardo P. S. M. Lobo,[‡] Ganesanpotti Subodh,^{||}
Mailadil T. Sebastian,^{||} Franklin M. Matinaga,[†] and Anderson Dias[⊥]

Departamento de Física, Instituto de Ciências Exatas, Universidade Federal de Minas Gerais, CP 702, Belo Horizonte MG 30123-970, Brazil; Laboratoire Photons et Matière (UPR 5 CNRS), ESPCI, Université Pierre et Marie Curie, 75231 Paris Cedex 5, France; Materials and Minerals Division, National Institute for Interdisciplinary Sciences and Technology, Trivandrum 695 019, India; and Departamento de Química, Instituto de Ciências Exatas e Biológicas, Universidade Federal de Ouro Preto, Ouro Preto MG 35400-000, Brazil

Received August 30, 2007. Revised Manuscript Received October 19, 2007

$\text{Sr}_{1-3x/2}\text{Ce}_x\text{TiO}_3$ dielectric ceramics (with x varying from 0.133 to 0.400) were investigated by Raman and infrared spectroscopies. The observed features could be related to SrTiO_3 phonon modes. The Raman spectra show first-order modes—which are modes either activated by polar defects or due to local symmetry lowering—together with classical second-order modes of SrTiO_3 . The infrared spectra are dominated by the three predicted polar phonons of SrTiO_3 , although a faint tetragonal distortion confirmed by low-temperature measurements was observed for all compositions. For increasing Ce content, the infrared spectra show a continuous hardening of the TO modes and the softening of the highest frequency LO mode. Together with the broadening of the TO phonon lines, these phonon energy evolutions explain the observed dielectric behavior of the material: namely, the decreasing of the dielectric constant and temperature coefficient of the resonance frequency (τ_f) with x . The quality factor is maximized for $x = 0.25$. Compared to pure SrTiO_3 , chemically substituted $\text{Sr}_{1-3x/2}\text{Ce}_x\text{TiO}_3$ ceramics present more adequate dielectric properties at microwave frequencies for technological applications.

Introduction

In the past three decades, telecommunications experienced an enormous advance due to the progress in wireless and microelectronic systems, in particular after the introduction of new devices and components operating at microwave (MW) frequencies. Dielectric resonator (DR) materials with high dielectric constant (ϵ_r), high-unloaded quality factor (Q_u), and low-temperature coefficient of resonant frequency (τ_f) play a key role in MW circuitry.^{1–5} Communication systems operating in the MW frequency range require low-loss and high dielectric constant ($\epsilon_r > 20$) materials as basic components in oscillators, filters, and antennas.^{6,7} Such materials ensure better performance along with reduction of weight and overall dimensions of the MW devices.^{5,8} However, as a general trend, by increasing the dielectric permittivity, Q_u decreases and τ_f increases.^{5,6} Therefore, the

development of MW ceramics with adequate dielectric properties for specific applications is a challenging problem in DR materials research.

Centrosymmetrical SrTiO_3 (ST) and CaTiO_3 (CT) present very high room temperature ϵ_r values in the MW region (290 and 162, respectively), owing to their incipient ferroelectric character.^{9,10} However, these materials have relatively high positive τ_f (1650 ppm/°C for ST and 859 ppm/°C for CT) and moderate losses ($Q_u \times f = 3000$ and 13 000 GHz for ST and CT in ceramic form, respectively) in that region.^{11–13} Therefore, polytitanate and solid solutions based on ST and CT materials are currently being investigated in order to tailor the dielectric properties, aiming to reduce the losses and to increase the thermal stability, while maintaining relatively high dielectric constants ($\epsilon_r > 100$).^{6,11–15} It is worthy noticing, however, that despite the practical interest in the macroscopic dielectric response of such systems, the obtained materials may present multiple phases.^{6,11–17} This is par-

* Corresponding author: Tel 55-31-3499-5624; e-mail bmoreira@fisica.ufmg.br.

[†] Universidade Federal de Minas Gerais.

[‡] Université Pierre et Marie Curie.

^{||} National Institute for Interdisciplinary Sciences and Technology.

[⊥] Universidade Federal de Ouro Preto.

- (1) Wersing, W. *Curr. Opin. Solid State Mater. Sci.* **1996**, *1*, 715.
- (2) Vanderah, T. A. *Science* **2002**, *298*, 1182.
- (3) Higuchi, Y.; Tamura, H. *J. Eur. Ceram. Soc.* **2003**, *23*, 2683.
- (4) Cava, R. J. *J. Mater. Chem.* **2001**, *11*, 54.
- (5) Nenasheva, E. A.; Kартенко, N. F. *J. Eur. Ceram. Soc.* **2001**, *21*, 2697.
- (6) Sebastian, M. T.; Santha, N.; Bijumon, P. V.; Axelsson, A. K.; Alford, N. M. *J. Eur. Ceram. Soc.* **2004**, *24*, 2583.
- (7) Sebastian, M. T.; Ohsato, H. *Mater. Integr.* **2005**, *18*, 6.
- (8) Fiedziuszko, S. J.; Hunter, I. C.; Itoh, T.; Kobayashi, Y.; Nishikawa, T.; Snitzer, S. N.; Wakino, K. *IEEE Trans. Microwave Theory Tech.* **2002**, *50*, 706.

- (9) Müller, K. A.; Burkard, H. *Phys. Rev. B* **1979**, *19*, 3593.
- (10) Lemanov, V. V.; Sotnikov, A. V.; Smirnova, E. P.; Weihnacht, M.; Kunze, R. *Solid State Commun.* **1999**, *110*, 611.
- (11) Wise, P. L.; Reaney, I. M.; Lee, W. E.; Price, T. J.; Iddles, D. M.; Cannell, D. S. *J. Eur. Ceram. Soc.* **2001**, *21*, 1723.
- (12) Wu, L.; Chen, Y. C.; Chen, L. J.; Chou, Y. P.; Tsai, Y. T. *Jpn. J. Appl. Phys.* **1999**, *38*, 5612.
- (13) Chen, X. M.; Li, L.; Liu, X. Q. *Mater. Sci. Eng., B* **2002**, *99*, 255.
- (14) Okawa, T.; Kiuchi, K.; Okabe, H.; Ohsato, H. *Jpn. J. Appl. Phys.* **2001**, *40*, 5779.
- (15) Sreemoolanadhan, H.; Sebastian, M. T.; Ratheesh, R.; Blachnik, R.; Woehlecke, M.; Schneider, B.; Neumann, M.; Mohanan, P. *J. Solid State Chem.* **2004**, *177*, 3995.
- (16) Ohsato, H. *J. Eur. Ceram. Soc.* **2001**, *21*, 2703.

ticularly true for the promising DR materials of the Ba–Ln₂O₃–TiO₂ system (Ln = lanthanide), where several secondary phases were identified.^{15–17} Conversely, it seems that polytitanate materials with appropriate amounts of Sr²⁺ and Ln³⁺ can crystallize in the perovskite structure, without any detectable secondary phase.^{18–22} In recent works, we have investigated the structure and dielectric properties of chemically substituted Sr_{1-3x/2}Ce_xTiO₃ ceramics, for x ranging from 0.133 to 0.400.^{20,22} The results showed that these materials crystallize in a perovskite cubic or pseudocubic structure, very similar to SrTiO₃. The calculated tolerance factors and the behavior of τ_f —which decreases with x but remains positive for increasing Ce contents—would also be in agreement with a cubic structure. In order to confirm the proposed crystalline structure and to investigate the phonon contributions to the dielectric response of Sr_{1-3x/2}Ce_xTiO₃ ceramics, we have undertaken a Raman and infrared study in these materials. Once ST has no Raman-active fundamental,²³ the presence of first-order phonons in the Raman spectra constitutes a good probe to detect any secondary phase or phase transitions to lower symmetry structures. Besides, the infrared spectra allow us to discuss the role of Ce substitution on the polar phonon modes of the system.

Experimental Section

Sr_{1-3x/2}Ce_xTiO₃ ceramics (0.133 ≤ x ≤ 0.400) were prepared by the solid-state ceramic route. The starting materials used were high-purity SrCO₃ and TiO₂ (99.9+%, Aldrich Chemical Co., Inc., Milwaukee, WI) and CeO₂ (99.99%, Indian Rare Earth Ltd., Udyogamandal, India). Stoichiometric amounts of powder mixtures (based upon the cation amounts) were ball-milled in distilled water medium using yttria-stabilized zirconia balls in a plastic container for 24 h. The slurry was dried, ground, and calcined at 1100 °C for 5 h. Cylindrical pucks containing 4 wt % poly(vinyl alcohol) as binder with around 7 mm height and 14 mm diameter were made by applying a pressure of 100 MPa. These compacts were then fired at 600 °C, for 30 min, to burn the binder before sintering in air at temperatures ranging from 1300 to 1400 °C for 2 h. Under these sintering conditions, Ce⁴⁺ reduces to Ce³⁺, producing the perovskite Sr_{1-3x/2}Ce_xTiO₃ materials.²² The final sintering temperature was determined for optimizing the dielectric properties of each sample. The higher this temperature was, the lower the residual amount of Ce⁴⁺ in the sample, as noticed in Table 1. Structural and microstructural characterizations (by XRD, SEM, and XPS) besides a detailed MW properties determination of the samples studied here were presented in detail in ref 22.

Optical spectroscopic measurements were done in samples previously polished to optical grade (down to 0.25 μm diamond paste). Micro-Raman scattering spectra were collected using a Jobin-Yvon T64000 spectrometer, equipped with a liquid-N₂-cooled CCD

Table 1. Chemical, Structural, and Microwave (2 GHz) Dielectric Parameters of Sr_{1-3x/2}Ce_xTiO₃ Ceramics (See Also Ref 22)^a

x	sintering T (°C)	Ce ⁴⁺ / Ce _{total}	a (Å)	V_m (Å ³)	α (Å ³)	ϵ_r CM	ϵ_r MW	$Q_{10}xf$ (GHz)	τ_f (ppm/°C)
0.400	1300	0.10	3.878	58.320	12.78	34.6	113	8000	306
0.333	1375	0.07	3.879	58.366	12.87	37.2	123	10000	392
0.286	1375	0.07	3.884	58.592	12.91	37.1	136	10800	428
0.250	1375	0.06	3.887	58.728	12.95	37.5	143	11000	478
0.222	1375	0.06	3.890	58.863	12.98	37.4	150	9600	497
0.200	1375	0.08	3.891	58.909	12.99	37.6	157	9300	544
0.182	1375	0.05	3.892	58.955	13.02	38.2	167	8000	601
0.167	1375	0.05	3.893	58.955	13.04	38.8	173	7800	637
0.154	1400	0.04	3.893	58.991	13.05	39.0	179	8000	724
0.143	1400	0.04	3.894	59.050	13.06	38.9	185	6000	789
0.133	1400	0.03	3.894	59.064	13.08	39.3			
0			3.905	59.547	13.20	40.0	290	3000	1650

^a $x = 0$ accounts for a SrTiO₃ single crystal. CM are the calculated Clausius–Mosotti dielectric constants.

detector and an Olympus microscope (50× objective). The measurements were done in backscattering geometry using the second harmonic line of a YVO₄:Nd laser (Coherent Verdi V6) as excitation source (532 nm, 5 mW at the sample's surface). A Notch filter cutting below 80 cm⁻¹ was used to stray light rejection. Accumulation times were typically five collections of 60 s, and the spectral resolution was better than 2 cm⁻¹.

Room-temperature infrared-reflectivity spectra were recorded on a Bruker IFS66v Fourier-transform spectrometer equipped with a homemade specular reflectance setup (external incidence angle of 8°). The far-infrared range (25–650 cm⁻¹) was studied by using a mercury-arc lamp, a 6 μm Ge-coated Mylar beamsplitter, and liquid-He-cooled Si bolometer. In the mid-infrared region (500–4000 cm⁻¹), a globar source (SiC), a Ge-coated KBr beamsplitter, and a pyroelectric DTGS detector were used. A gold mirror was used as reference. Low-temperature measurements, from 300 K down to 5 K, were carried out in a homemade continuous flow cryostat with the sample in He vapor. The cryostat was equipped with polypropylene windows for the far-infrared and ZnSe for the mid-infrared. The resolution was maintained at 2 cm⁻¹. For sake of comparison, infrared spectra of a well-polished SrTiO₃ single crystal (CrysTec GmbH) were also obtained.

Results and Discussion

As stated in the Introduction, XRD patterns of chemically substituted Sr_{1-3x/2}Ce_xTiO₃ materials ($x \leq 0.400$) show a cubic or pseudocubic ST-like structure, with no secondary phase detected.^{20,22} Since ST belongs to the $Pm\bar{3}m$ structure, with no Raman-active fundamental,²³ we have used Raman spectroscopy to reinvestigate the structure of our samples. Figure 1 presents the Raman spectra of Sr_{1-3x/2}Ce_xTiO₃ samples for several x values, which show a relatively high quasielastic scattering together with rather broad Raman peaks. We note first the high similarity between the spectra of the different samples, from $x = 0.133$ to 0.400, which is an indicative that all samples belong to the same crystal space group, irrespective of the Ce content. Besides the high quasielastic wing, 10 inelastic features can be identified in the spectra. These features have been indicated in Figure 1, where we have also pointed out their possible origins, according to the literature data on pure, cation-doped or nanocrystalline ST samples.^{24–31}

- (17) Solomon, S.; Santha, N.; Jawahar, I. N.; Sremoolanadhan, H.; Sebastian, M. T.; Mohanan, P. *J. Mater. Sci. Mater. Electron.* **2000**, *11*, 595.
- (18) Bamberger, C. E.; Haverlock, T. J.; Kopp, O. C. *J. Am. Ceram. Soc.* **1994**, *77*, 1659.
- (19) Howard, C. J.; Lumpkin, G. R.; Smith, R. I.; Zhang, Z. *J. Solid State Chem.* **2004**, *177*, 2726.
- (20) Subodh, G.; Sebastian, M. T. *Mater. Sci. Eng., B* **2007**, *136*, 50.
- (21) Almeida, A.; Correia, T. M.; Chaves, M. R.; Vilarinho, P. M.; Kholkin, A. L.; Costa, A. M. *J. Eur. Ceram. Soc.* **2007**, *27*, 3701.
- (22) Subodh, G.; James, J.; Sebastian, M. T.; Paniago, R.; Dias, A.; Moreira, R. L. *Chem. Mater.* **2007**, *19*, 4077.
- (23) Nilsen, W. G.; Skinner, J. G. *J. Chem. Phys.* **1968**, *48*, 2240.

- (24) Tkach, A.; Vilarinho, P. M.; Kholkin, A. L.; Pashkin, A.; Samoukhina, P.; Pokorny, J.; Veljko, S.; Petzelt, J. *J. Appl. Phys.* **2005**, *97*, 044104.

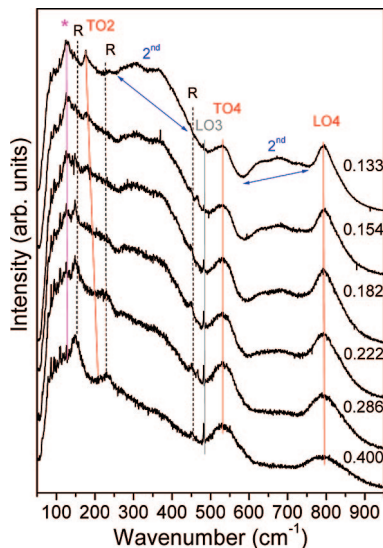


Figure 1. Room-temperature (RT) Raman spectra of $\text{Sr}_{1-3x/2}\text{Ce}_x\text{TiO}_3$ ceramics, for x ranging from 0.133 to 0.400. The spectra are vertically upshifted for sake of clarity. The tentative assignments of the main features are indicated. Besides the second-order modes, infrared (TO₂, TO₄, LO₄), silent (LO₃), R-point modes and an impurity-related mode (*) were identified.

The similarity between the Raman spectra of our samples for different x as well as with small-sized or doped SrTiO_3 is very strong. At the Brillouin zone center, cubic ST crystals present three optical polar modes of F_{1u} symmetry (historically known as modes 1, 2, and 4), which are infrared-active, one silent mode of F_{2u} symmetry (named mode 3), besides the acoustic degenerate mode (F_{1u}).^{32–34} These modes are forbidden in the Raman spectra by selection rules, which strictly hold for pure crystalline systems only. The presence of defects as well as size effects can relax the symmetry rules and activate these fundamental modes in the Raman spectrum, as shown recently for several ST-based materials.^{24–31} In the case of our chemically substituted $\text{Sr}_{1-3x/2}\text{Ce}_x\text{TiO}_3$ ceramics, although the average crystalline structure appear to remain cubic, Ce ions and their associated vacancies—sharing the perovskite A-sites with Sr ions—are responsible for a local symmetry breaking, relaxing the selection rules. Therefore, first-order fundamentals could become active,

similarly to what was observed in Mg-doped ST.²⁴ This is the case of the broad features located around 177, 530, and 795 cm^{-1} in Figure 1, whose characteristics allow us to assign them as the infrared TO₂, TO₄, and LO₄ modes of ST, respectively.^{27,31–33} Because these modes are polar, they would be intrinsically broad in Raman spectra of polycrystalline samples due to frequency dependences with phonon propagation direction (oblique phonons). The additional broadening of these modes with increasing Ce contents is likely due to the increasing disorder of the system. The hardening and the weakening of the TO₂ mode are also noticeable. Another forbidden first-order cubic mode was activated by symmetry breaking: the very sharp band at 483 cm^{-1} , whose intensity increases with x . This feature can be assigned to the silent LO₃ mode (F_{2u} symmetry), also observed in hetero- or small-sized ST systems.^{29–31,33} Conversely to the polar F_{1u} modes, the F_{2u} nonpolar mode remains narrow with increasing Ce content (no dispersion with propagation direction, absence of electrostatic interaction with defects).

Three other features also seem to come from first-order scattering (bands indicated by R in Figure 1), located at 148, 235, and 453 cm^{-1} . These bands become strong with x and were also observed by other authors in cation-doped and low-dimension ST-based materials.^{24–28,31} According to these authors, they probably correspond to first-order vibrations at the R point ($1/2, 1/2, 1/2$) of the Brillouin zone, which, in principle, should not be accessible by optical techniques. Nevertheless, local elastic distortions of the cubic cell can activate these modes by partially (and eventually, completely) folding the Brillouin zone. Indeed, pure ST crystals present an antiferrodistortive phase transition to the tetragonal $I4/mcm$ structure below ca. 110 K,^{24,34–39} with the appearing of five Raman characteristic fundamentals at 16, 26, 146, 236, and 450 cm^{-1} (at 120 K, for a polycrystalline sample).³⁸ It is worth noticing that the presence of defects or impurities increases this transition temperature. For instance, in the mixed $\text{Sr}_{0.70}\text{Ca}_{0.30}\text{TiO}_3$ perovskite the cubic-to-tetragonal transition occurs at 230 K.²⁸ The presence and intensity behavior of the tetragonal first-order features in our Raman spectra seem to indicate an increasing tetragonal distortion of the “average” cubic cells (possibly due to short-range cation ordering), rather than a complete phase transition for large x . This observation is consistent with the behavior of the classical cubic second-order Raman modes,²³ which appear in the regions 260–450 and 590–750 cm^{-1} (very broadband envelopes indicated by “2nd” in Figure 1) and tend to vanish for increasing Ce content. A possible scenario would be the smearing and continuous increasing of the critical temperature with x , which could lead to some phase coexistence at room temperature, with predominance of the cubic phase. Finally, we point out the presence of a low-frequency Raman band (asterisk at 125 cm^{-1}), which is

- (25) Sirenko, A. A.; Akimov, I. A.; Fox, J. R.; Clark, A. M.; Li, H. C.; Si, W.; Xi, X. X. *Phys. Rev. Lett.* **1999**, *82*, 4500.
 (26) Banerjee, S.; Kim, D.-I.; Robinson, R. D.; Herman, I. P.; Mao, Y.; Wong, S. S. *Appl. Phys. Lett.* **2006**, *89*, 223130.
 (27) Petzelt, J.; Ostapchuk, T.; Gregora, I.; Savinov, M.; Chvostova, D.; Liu, J.; Shen, Z. J. *Eur. Ceram. Soc.* **2006**, *26*, 2855.
 (28) Oullon, R.; Pinan-Lucarre, J.-P.; Ranson, P.; Pruzan, Ph.; Mishra, S. K.; Ranjan, R.; Pandey, Dh. *J. Phys.: Condens. Matter* **2002**, *14*, 2079.
 (29) Du, Y.-L.; Guang, C.; Zhang, M.-S.; Yang, S.-Z. *Chin. Phys. Lett.* **2003**, *20*, 1561.
 (30) Tenne, D. A.; Bruchhausen, A.; Lanzillotti-Kimura, N. D.; Fainstein, A.; Katiyar, R. S.; Cantarero, A.; Soukiassian, A.; Vaithyanathan, V.; Haeni, J. H.; Tian, W.; Schlom, D. G.; Choi, K. J.; Kim, D. M.; Eom, C. B.; Sun, H. P.; Pan, X. Q.; Li, Y. L.; Chen, L. Q.; Jia, Q. X.; Nakhmanson, S. M.; Rabe, K. M.; Xi, X. X. *Science* **2006**, *313*, 1614.
 (31) Petzelt, J.; Ostapchuk, T.; Gregora, I.; Kuzel, P.; Liu, J.; Shen, Z. J. *Phys.: Condens. Matter* **2007**, *19*, 196222.
 (32) Spitzer, W. G.; Miller, R. C.; Kleinman, D. A.; Howarth, L. E. *Phys. Rev.* **1962**, *126*, 1710.
 (33) Almeida, B. G.; Pietka, A.; Caldelas, P.; Mendes, J. A.; Ribeiro, J. L. *Thin Solid Films* **2006**, *513*, 275.
 (34) Fleury, P. A.; Scott, J. F.; Worlock, J. M. *Phys. Rev. Lett.* **1968**, *21*, 16.

- (35) Müller, K. A. *Phys. Rev. Lett.* **1959**, *2*, 341.
 (36) Unoki, H.; Sakudo, T. *J. Phys. Soc. Jpn.* **1967**, *23*, 546.
 (37) Taylor, W.; Murray, A. F. *Solid State Commun.* **1979**, *31*, 937.
 (38) Balachandran, U.; Eror, N. G. *J. Am. Ceram. Soc.* **1982**, *65*, C54.
 (39) Ostapchuk, T.; Petzelt, J.; Zelezny, V.; Pashkin, A.; Pokorný, J.; Drbohlav, I.; Kuzel, R.; Rafaja, R.; Gorshunov, B. P.; Dressel, M.; Ohly, Ch.; Hoffmann-Eifert, S.; Waser, R. *Phys. Rev. B* **2002**, *66*, 235406.

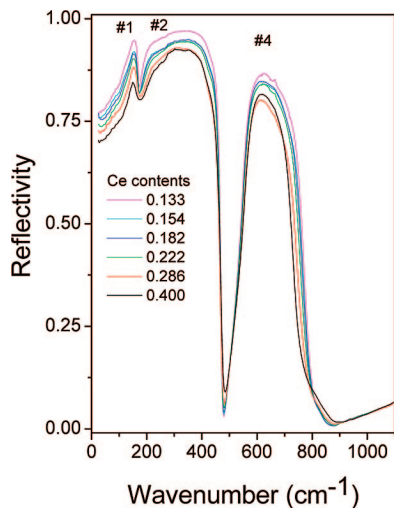


Figure 2. RT infrared-reflectivity spectra of Sr_{1-3x/2}Ce_xTiO₃ solid solution in the 25–1100 cm⁻¹ spectral region, for the same samples as in Figure 1. The three cubic SrTiO₃ modes are indicated by their historical numbers.

attributed to a polar-impurity induced band in the cubic phase.²⁸ This band weakens for increasing x values, which is in agreement with the proposed distortion of the cubic phase.

In order to confirm the above attributions of the defect-activated Raman fundamentals as well as the assumed locally distorted cubic symmetry of the materials, we have investigated their infrared-reflectivity spectra. The experimental data for some representative samples (the same as in Figure 1) are presented in Figure 2. The visual inspection of the spectra shows three well-defined modes for all samples, whose origin would be the same as in cubic ST: #1 assigned to Ti–O–Ti bending; #2 related to A–TiO₆ translations; and #4 due to Ti–O stretching.^{33,39} Notice the high similarity between the spectra of different samples, confirming their average cubic symmetry and the absence of clear phase transitions due to the introduction of Ce ions. However, a careful inspection of this figure reveals the presence of a faint anomaly in the reflectivities around 430 cm⁻¹ and also a shoulder just above 800 cm⁻¹, which increase for increasing Ce contents. Once the cubic-to-tetragonal transition of ST is marked by the appearing of a dip in the reflectivity spectra at around 438 cm⁻¹,^{27,40} which could be related to the 430 cm⁻¹ anomaly seen here at room temperature, we have undertaken low-temperature measurements in our samples.

Figure 3a,b presents the low-temperature infrared-reflectivity spectra for the samples with (a) $x = 0.133$ and (b) 0.400 down to 5 K. In both cases, we note that the only appreciable changes with temperature are the increasing of overall reflectivity (with more important consequences for the lower frequency limit because of the softening of TO₁ mode) and the enhancement of the tetragonal dip centered at 429 cm⁻¹. Conversely to ST, where this dip appears only below 110–120 K, our solid solution samples presented the dip even at room temperature, although a clear evolution appeared only around 200 K (see insets in Figure 3a,b). This result confirms the previous Raman observation of the

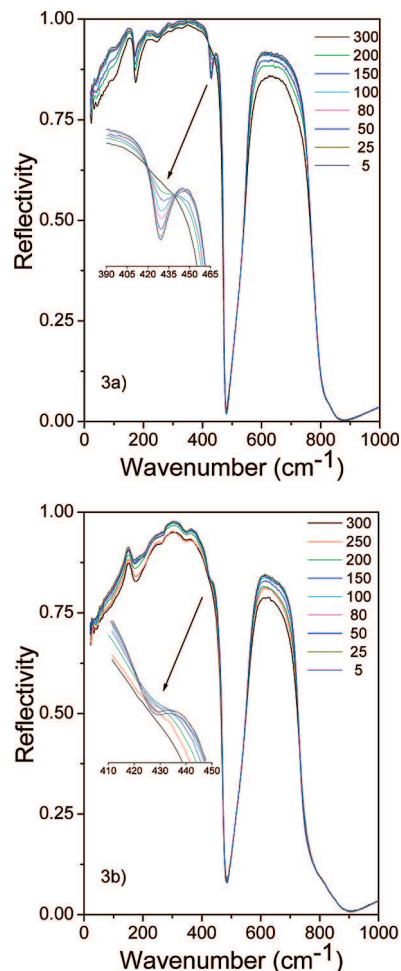


Figure 3. Low-temperature infrared-reflectivity spectra of Sr_{1-3x/2}Ce_xTiO₃ for (a) $x = 0.133$ and (b) 0.400. The temperatures (K) are indicated. The insets show details around the dip characterizing the cubic-to-tetragonal SrTiO₃ phase transition.

existence of a tetragonal distortion of the average cubic phase and also the rising of the cubic-to-tetragonal phase transition temperature (above 200 K) for our samples with $0.133 \leq x \leq 0.400$. Concerning the shoulder around 800 cm⁻¹, Figure 3a,b shows that this feature presents no evolution with temperature down to 5 K. Therefore, it is linked neither to the ST tetragonal phase nor to the ST cubic one. Although this feature becomes more intense with x , it should be a defect (impurity) mode, rather than due to a secondary phase. Our Raman spectra only detected ST-like modes, although the higher frequency band assigned to LO₄ phonon (Figure 1) could be superimposed to this 800 cm⁻¹ defect mode.

The classical Lorentz phonon dispersion is well-known not to describe the IR spectra of SrTiO₃.³² Therefore, we utilized the four-parameter semiquantum model⁴¹ to obtain the phonon characteristics of the room-temperature IR modes of our compounds. This model gives a unique solution for spectra obtained for cubic systems or with polarized light along the crystal principal axes for lower symmetry structures. For other polycrystalline or unoriented material, a

(41) Gervais, F.; Echegut, P. In *Incommensurate Phases in Dielectrics*; Blinc, R., Levanyuk, A. P., Eds.; North-Holland: Amsterdam, 1986; p 337.

(40) Galzerani, J. C.; Katiyar, R. S. *Solid State Commun.* **1982**, *41*, 515.

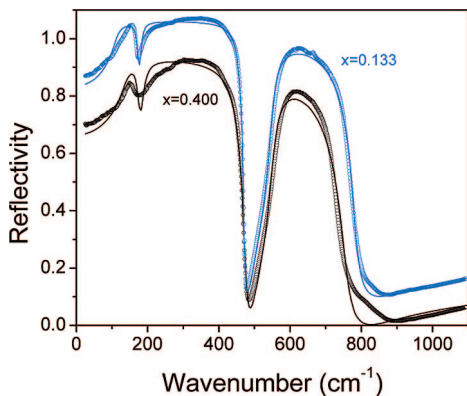


Figure 4. Experimental (circles) and adjusted (solid lines) infrared reflectivity spectra (RT) of $\text{Sr}_{1-3x/2}\text{Ce}_x\text{TiO}_3$ ceramic samples for $x = 0.133$ and 0.400 . The spectrum of $x = 0.133$ is vertically up-shifted (+0.1) for clarity. Three phonon modes of the cubic structure were used for the fittings.

Table 2. Polar-Phonon Fitting Frequencies and Infrared Dielectric Parameters for $\text{Sr}_{1-3x/2}\text{Ce}_x\text{TiO}_3$ Ceramics and SrTiO_3 Single Crystal ($x = 0$)

x	TO_1 (cm^{-1})	LO_1 (cm^{-1})	TO_2 (cm^{-1})	LO_2 (cm^{-1})	TO_4 (cm^{-1})	LO_4 (cm^{-1})	ϵ_0	$Q_{\omega}f$ (THz)
0.400	139.8	177.4	189.1	475.8	551.9	756.2	97	20.3
0.333	131.5	178.3	187.7	473.4	552.9	761.7	114	18.1
0.286	128.1	179.8	189.5	472.6	551.8	768.5	118	14.2
0.250	127.1	180.6	189.6	471.9	552.3	770.7	124	16.5
0.222	124.7	176.3	184.8	471.6	551.4	773.0	132	16.0
0.200	121.6	177.2	186.1	471.5	551.3	774.3	137	13.1
0.182	119.7	176.1	184.1	471.4	550.7	776.0	146	14.7
0.167	118.3	175.2	183.3	471.3	550.6	776.9	148	13.5
0.154	114.6	176.0	183.3	471.3	549.8	778.2	157	12.4
0.143	115.3	175.9	182.4	471.2	550.8	779.4	161	15.7
0.133	112.8	175.2	181.0	471.2	549.9	780.4	171	17.1
0	92.4	171.0	173.9	475.0	545.0	795.8	297	19.1

unique solution (concerning all phonon positions and widths) is obtained when there is no overlap between TO–LO pairs belonging to different irreducible representations. Figure 4 presents the experimental data and the corresponding obtained fitting curves for $x = 0.133$ and 0.400 . A summary of the fitting parameters for all measured samples, including a SrTiO_3 single crystal, is presented in Table 2. It is clear from Figure 4 that there would be at least two missing modes in the fittings to perfectly account for the total reflectivity. If we use four or five bands for the fitting, apparent good matching for the curves are obtained, though through physically unsound positions and widths. Indeed, in the present case, the observed 800 cm^{-1} feature (longitudinal value) certainly overlaps with the fourth cubic mode (the transversal frequency of this mode is below the LO_4 position). It seems also that there would be a low-frequency mode overlapping with the cubic modes 1 and 2. By trying to add a low-frequency mode to the fit, we completely lose the information about the important TO_1 mode. We can conclude that the missing modes have different symmetries than the cubic ones, so that we cannot resolve them unambiguously for our system. We remark that even in crystalline SrTiO_3 the tetragonal A_{2u} and E_u modes are not resolved because of the existence of multiple ferroelastic domains.

The variations of the adjusted infrared frequencies of the cubic modes of $\text{Sr}_{1-3x/2}\text{Ce}_x\text{TiO}_3$ with Ce concentration are

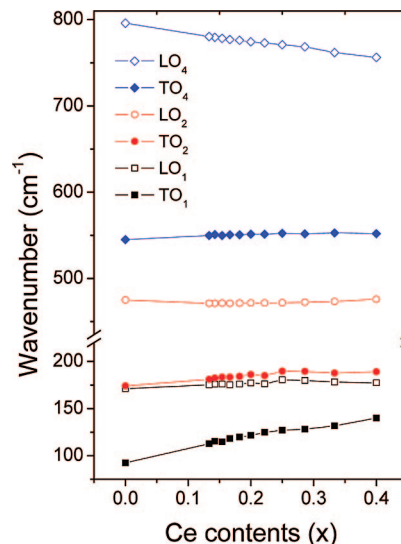


Figure 5. Variations of the cubic phonon frequencies at RT for $\text{Sr}_{1-3x/2}\text{Ce}_x\text{TiO}_3$ as functions of Ce contents (x). Experimental values for SrTiO_3 ($x = 0$) are included.

shown in Figure 5. Data of pure SrTiO_3 crystal are included for comparison. It is seen that all TO modes harden with increasing x , which can be attributed to the interaction of the corresponding phonon modes with polar defects (i.e., Ce^{4+} and, maybe, Ce^{3+} acting as a defect and polar vacancies).^{42,43} The effect of Ce substitution on the longitudinal LO_1 and LO_2 modes is very weak. On the other hand, the LO_4 mode softens with the presence of such defects, which shows a strong electrostatic interaction between the polar defects and the longitudinal polar phonon branch linked to Ti–O stretching mode. The hardening of the TO_2 mode is also observed in the Raman spectra of Figure 1, although the corresponding band tends to vanish with increasing Ce contents due to the increasing disorder in the system. On the other hand, the broadening of Raman features corresponding to the defect-activated TO_4 and LO_4 bands masks the variations of their peak centers with x .

The variations of the phonon frequencies and widths determine the MW dielectric behavior of the $\text{Sr}_{1-3x/2}\text{Ce}_x\text{TiO}_3$ system. Indeed, the high dielectric constant of SrTiO_3 is originated mainly from the behavior of its lower frequency TO_1 mode, which softens by decreasing the temperature, although this material does not present a ferroelectric transition due to zero-point quantum fluctuations—a characteristic that led it to be classified as an incipient ferroelectric.^{9,10} Because of that, the room-temperature dielectric constant of ST (ca. 300 at $20\text{ }^\circ\text{C}$) is much higher than the $\epsilon_r = 40.0$ value calculated from the Shannon's additive polarizability rule (via the Clausius–Mosotti equation) for determining dielectric constants in centrosymmetric oxides.⁴⁴ We have calculated the predicted dielectric constants from this method for our ceramics using the average

(42) Crandles, D. A.; Nicholas, B.; Dreher, C.; Holmes, C. C.; McConnell, A. W.; Clayman, B. P.; Gong, W. H.; Greedan, J. E. *Phys. Rev. B* **1999**, *59*, 12842.

(43) Sirenko, A. A.; Bernhard, C.; Golnik, A.; Clark, A. M.; Hao, J.; Si, W.; Xi, X. X. *Nature (London)* **2000**, *404*, 373.

(44) Shanon, R. D. *J. Appl. Phys.* **1993**, *73*, 348.

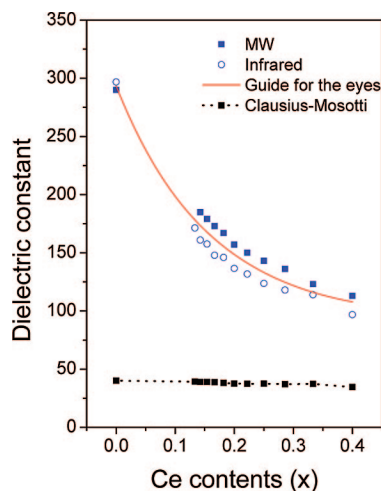


Figure 6. Dependence of the extrinsic (MW) and intrinsic (infrared) relative dielectric constants of the Sr_{1-3x/2}Ce_xTiO₃ as functions of the Ce contents (x) at RT. SrTiO₃ values are included.

polarizabilities (α) for the A-site ions and the measured molecular volumes ($V_m = a^3$; see Table 1). The results are presented in Figure 6, together with the measured MW dielectric constants (see also Table 1) and the infrared intrinsic values (called here ϵ_0), obtained from the Lydane–Sachs–Teller relationship⁴¹

$$\epsilon_0 = \epsilon_\infty \prod_{j=1}^N \frac{\Omega_{j,LO}^2}{\Omega_{j,TO}^2} \quad (1)$$

where N is the number of polar phonons, ϵ_∞ is the high-frequency dielectric constant due to the electronic polarization contribution, and $\Omega_{j,LO}$ ($\Omega_{j,TO}$) is the longitudinal (transverse) optical frequency of the j th polar mode. We note that the observed dielectric constants of all materials present a large deviation from the Shannon's prediction, showing that Sr_{1-3x/2}Ce_xTiO₃ materials are also incipient ferroelectrics and that the decreasing of their dielectric constants with x is mainly determined by the hardening of their soft phonon mode by influence of Ce ions and associated vacancies. (The hardening of the other TO modes and the softening of the LO₄ mode have a lower contribution for this behavior.)

The results obtained for the intrinsic dielectric constant (ϵ_0) are very close but smaller than those obtained by direct MW measurements. Although the latest values could have some extrinsic contribution (space charges and polarizable grain boundaries), the most probable reason for this difference is that the infrared values were underestimated, once not all polar modes were taken into account during fitting. In spite of that, the phonon-driven dielectric behavior of the mixed system is very clear. On the other hand, since we only considered the strongest modes, the losses were underestimated and, thus, the intrinsic (phonon) quality factors, $Q_u = (\tan \delta)^{-1}$, overestimated. The latest values are calculated from the TO phonon parameters by⁴¹

$$\tan \delta = \sum_j \tan \delta_j = \sum_j \omega \frac{\Delta \epsilon_j \gamma_{j,TO}}{\epsilon_0 \Omega_{j,TO}^2} \quad (2)$$

where $\Delta \epsilon_j$ is the oscillator strength and $\gamma_{j,TO}$ the damping of the j th mode. The infrared quality factors (Table 2) are 2 or

3 times larger than the MW ones (Table 1) because the extrapolation of the infrared losses to the MW region is often spoiled due to the dominance of extrinsic losses of different origins (polar species, microstructural defects, etc.), leading to overestimated quality factors.⁴⁵ In spite of that, we believe that the maximum $Q_u x f$ value observed at 2 GHz for the sample with $x = 0.25$ is also driven by the phonon behavior; i.e., for increasing x there would be a competition between the hardening of the TO modes, responsible for the increasing of Q (increasing the Ω_{TO}) that is more important for lower x values, and the systematic broadening of the TO line widths (γ_{TO}) due to the disorder introduced in the system, which reduces the phonon lifetimes, becoming more important for higher x .

Finally, let us discuss the behavior of the temperature coefficient of the resonance frequency (τ_f), which was measured at 2 GHz (see Table 1). It is well established that this parameter is given by $\tau_f = -(\alpha_L + \tau_\epsilon/2)$, where α_L is the linear thermal expansion coefficient and τ_ϵ is the temperature coefficient of the dielectric constant.⁴⁶ For complex perovskite materials, α_L usually lies between 9 and 12 ppm/°C, so that we can assume that the thermal expansion contribution to τ_f for our ceramics are approximately the same for different x values (including ST), which has $\alpha_L = 10$ ppm/°C at room temperature.⁴⁷ Therefore, the high positive value of τ_f for ST is directly linked to the behavior of its soft mode, which leads to an important increase of ϵ_r with decreasing temperature, i.e., to a high (negative) temperature derivative of ϵ_r . In the Sr_{1-3x/2}Ce_xTiO₃ system, the monotonous hardening of the soft mode with increasing Ce content leads to the decreasing of ϵ_r and, then, to a consequent decreasing of $|\tau_\epsilon|$ and τ_f . Therefore, we conclude that the observed improvement of this parameter in our system (reduction by a factor of 5, if compared to ST) is also a direct consequence of the soft-mode behavior. Aiming to technological applications in the MW region, chemically substituted Sr_{1-3x/2}Ce_xTiO₃ represents an advance compared to pure SrTiO₃, since they present highly improved dielectric merit factors.

Conclusions

Raman and infrared spectra of Sr_{1-3x/2}Ce_xTiO₃ dielectric ceramics are well compatible with an average ideal cubic perovskite structure, for materials with x ranging from 0.133 to 0.400. The presence of polar defects in the A-site (Ce³⁺, Ce⁴⁺, and associated vacancies) relaxes the symmetry rules and activates first-order phonon modes (infrared-active cubic modes and modes of the Brillouin R-point folded into the zone center by local tetragonal distortion) in the Raman spectra. The infrared spectra are dominated by the three predicted ST polar phonons. Low-temperature spectra confirmed the local symmetry lowering and indicate the rising of the cubic-to-tetragonal ST-like transition temperature. The hardening of the polar TO modes and the softening of the higher frequency LO mode with increasing Ce content

(45) Petzelt, J.; Kamba, S. *Mater. Chem. Phys.* **2003**, *79*, 175.

(46) Colla, E. L.; Reaney, I. M.; Setter, N. *J. Appl. Phys.* **1993**, *74*, 3414.

(47) *Landolt-Börnstein*; Hellwege, K.-H., Hellwege, A. M., Eds.; Springer-Verlag: Berlin, 1981; Vol. 16, p 308.

are responsible for the observed dielectric behavior of the material: decreasing of dielectric constant and τ_f and increasing of quality factor. The measured dielectric properties are competitive to that of the existing high dielectric constant MW ceramics. Compared to pure SrTiO₃, Sr_{1-3x/2}Ce_xTiO₃ ceramics present more adequate dielectric properties at MW frequencies for technological applications.

Acknowledgment. The authors are grateful to MCT/CNPq, FINEP, and FAPEMIG (Brazil) and to the Department of Science and Technology, New Delhi (India), for partially

funding this work. G. Subodh is thankful to the Council of Scientific and Industrial Research (India) for a Junior Research Fellowship. Part of the IR work was performed while R.L.M. had an invited "Chaire Joliot" appointment at ESPCI.

Supporting Information Available: Room-temperature infrared-reflectivity spectra (experimental and adjusted curves with the four-parameter semiquantum model) for all samples, including ST single crystal, fitting parameters for the cubic phase, and experimental low-temperature spectra for ST are supplied. This material is available free of charge via the Internet at <http://pubs.acs.org>.

CM7024747